


Photocatalytic Degradation of Malachite Green Dye via An Inner Transition Metal Oxide-Based Nanostructure Fabricated through a Hydrothermal Route [†]

Sabeeha Jabeen ^{1,2}, Adil Shafi Ganie ³, Shashi Bala ² and Tahmeena Khan ^{1,*} 

¹ Department of Chemistry, Integral University, Lucknow 226026, India; saabeeha.habib@gmail.com

² Department of Chemistry, University of Lucknow, Lucknow 226007, India; shashichem15@gmail.com

³ Organic Chemistry Section, Department of Chemistry, University of Kashmir, Hazratbal 190006, India; aadilshafi1@gmail.com

* Correspondence: tahminakhan30@yahoo.com

[†] Presented at the 4th International Online Conference on Nanomaterials, 5–19 May 2023; Available online: <https://iocn2023.sciforum.net>.

Abstract: This experimentation focuses on an inner transition metal oxide-based nanostructure LaFeO₃ which was fabricated by a hydrothermal route for photocatalytic degradation of dye under visible light irradiation. The fabricated nanostructure was characterized by various techniques, including X-ray diffraction (XRD), which depicts the crystalline nature and size of the synthesized nanostructure which is 45 nm; Field emission scanning electron microscopy (FE-SEM), which determined the overall morphology of the nanocomposite; and energy dispersive X-ray (EDAX) analysis, which established the presence of La, O, and Fe in the sample. The photocatalytic activity of the samples was checked for the decolorization of malachite green (MG) dye. It was observed that the nanostructure showed maximum response with more than 80% degradation of MG in 80 min.

Keywords: malachite green dye; photocatalysis; LaFeO₃; perovskite; hydrothermal synthesis



Citation: Jabeen, S.; Ganie, A.S.; Bala, S.; Khan, T. Photocatalytic Degradation of Malachite Green Dye via An Inner Transition Metal Oxide-Based Nanostructure Fabricated through a Hydrothermal Route. *Mater. Proc.* **2023**, *14*, 5. <https://doi.org/10.3390/IOCN2023-14445>

Academic Editor: Antonio Di Bartolomeo

Published: 5 May 2023



Copyright: © 2023 by the authors. Licensee MDPI, Basel, Switzerland. This article is an open access article distributed under the terms and conditions of the Creative Commons Attribution (CC BY) license (<https://creativecommons.org/licenses/by/4.0/>).

1. Introduction

The materials having a size dimension in the nano-range exhibit outstanding physical and chemical properties as compared to the bulk material [1,2]. Nanostructured materials have received significant consideration because of their involvement in miscellaneous areas, i.e., drug development, farming, bioengineering, transport, nutrition supplements, devices, space, packing materials, fabric, microchip technology, and cosmetics industries [3–5]. Perovskites having general formula ABO₃ have shown to possess outstanding characteristics because of their unique structure and properties, such as electric conduction, insulator, ferroelectric, magnetic, thermochemical, and catalysis. Furthermore, these characteristic properties can be easily manipulated by changing the particular ratio of rare-earth ions A and B in the perovskite oxides [6,7]. The replacement of ions is the finest tactic to boost the efficient characteristics of the nanostructure, which can be exploited for new-generation nanostructure materials [8,9]. ABO₃-type mixed oxide perovskite nanostructures, such as LaMnO₃, LaNiO₃, PbTiO₃, and LaCrO₃, [10] have been recognized and, because of their tremendous photocatalytic activity, they are generally used as a photocatalyst in wastewater remediation applications [11,12]. The release of dangerous manufacturing wastes into the water bodies and air results in critical ecological problems [13]. Henceforth, it is compulsory to eradicate these dangerous ingredients before releasing them into the environment. The noxious ingredients produced from colorants can be eradicated via physiochemical tactics, such as co-precipitation, nano-photocatalysis, nano-adsorption, nanofiltration, and advanced oxidation processes [12]. A competent technique, such as photocatalysis, has appeared for the decontamination of wastewater. In the typical procedure, electron–hole pairs accumulated at the valence band and at the conduction band

are produced by band-gap energy, responsible for redox reactions with the recalcitrant adsorbed on the exterior of the nanophotocatalyst [13]. The reaction conditions, such as the pH of the reaction, the quantity of the photocatalyst, substrate concentration, and treatment time nanophotocatalytic performance have also been explored. Photocatalytic tactics are cast-off as a pre-treatment for the conversion of non-biodegradable organic contaminants to biodegradable compounds owning low molecular weight [14]. The linking of semiconductor photocatalysts shows greater photocatalytic capability, thus increasing the charge transfer and outspreading the energy range of photoexcitation [15].

This assessment is concentrated on the fabrication and characterization of the LaFeO_3 nanostructure fabricated through the hydrothermal route. The surface area and conductivity of LaFeO_3 can be enhanced by substituting the Fe metal ions in the ABO_3 lattice. The characterization of the prepared nanostructured material was performed by transmission electron microscopy (TEM) and scanning electron microscopy with energy-dispersive X-ray spectroscopy (SEM-EDS). The photocatalytic performance of the fabricated nanostructure was evaluated by means of the photodegradation of Malachite green dye. Malachite green dye is a dye used as an antifungal in ponds and lakes. It is cast-off in paper manufacturing, and in the cloth industry for dyeing silks [16]. It is a water-soluble dye and may be carcinogenic, and can cause chromosome disorders, and skin diseases [17]. The synthesized LaFeO_3 nanostructure degraded approximately 82% of the dye in 80 min only.

2. Materials and Methods

The Malachite dye used was purchased from Sigma Aldrich, (St. Louis, MO, USA). The photocatalysis tests were performed under visible light. The crystallinity and phase identification purity of the synthesized LaFeO_3 were detected by using a diffractometer (XRD, Rigaku Ultima IV, Tokyo, Japan). FTIR spectra were obtained using a spectrophotometer (Thermo Scientific Nicolet iS50 FTIR Tri-detector, Waltham, MA, USA). The morphology of the nanostructures was carried out by a Scanning Electron microscope (SEM) Zeiss Gemini SEM 500 with EDS detector, Singapore and the perovskite nanostructure was determined by Transmission electron microscope (TEM) (JOEL-JSM 6360, Tokyo, Japan).

Synthesis

The LaFeO_3 nanostructure was fabricated by the hydrothermal route using lanthanum nitrate, and ferric nitrate nonahydrate in equimolar amounts as a precursor and then dissolved in 40 mL double distilled water with continuous magnetic stirring followed by dropwise addition of NaOH to maintain pH. After strong stirring, the mixture was relocated into a Teflon-lined stainless autoclave and heated at 200 °C for 14 h [18–21]. The resultant precipitate was filtered, washed with DI water and ethanol, and then dried at 90 °C to obtain the dark-colored LaFeO_3 nanostructure powder. The photocatalytic activity of the LaFeO_3 nanostructures in the eradication and decomposition of Malachite dye was assessed at room temperature. For every trial, 30 mg of nanostructures was distributed in 60 mL of the Malachite dye solution.

3. Results and Discussion

3.1. Characterization

Figure 1a XRD depicts the crystalline nature and size of the synthesized nanostructure, which is 45 nm, calculated by the Debye Scherrer equation, all peaks matched well with JCPDS card no. 00-037-1493, as shown in Figure 1a. Figure 1b reveals the cubic morphology of the LaFeO_3 nanostructure, where the rough surface of the LaFeO_3 nanostructure is clearly visible [22] FTIR confirmed the fabrication of a metal oxide-based nanostructure via peaks between 4000 and 400 cm^{-1} as depicted in Figure 1c [23]. TEM images depicted in Figure 1d revealed the perovskite assembly of the synthesized nanostructure. EDX spectrum depicted in Figure 1e revealed the presence of La, O, and Fe elements in the synthesized nanostructure. The Tauc plot depicted in Figure 1f revealed the band gap energy which is 2.48 eV [24].

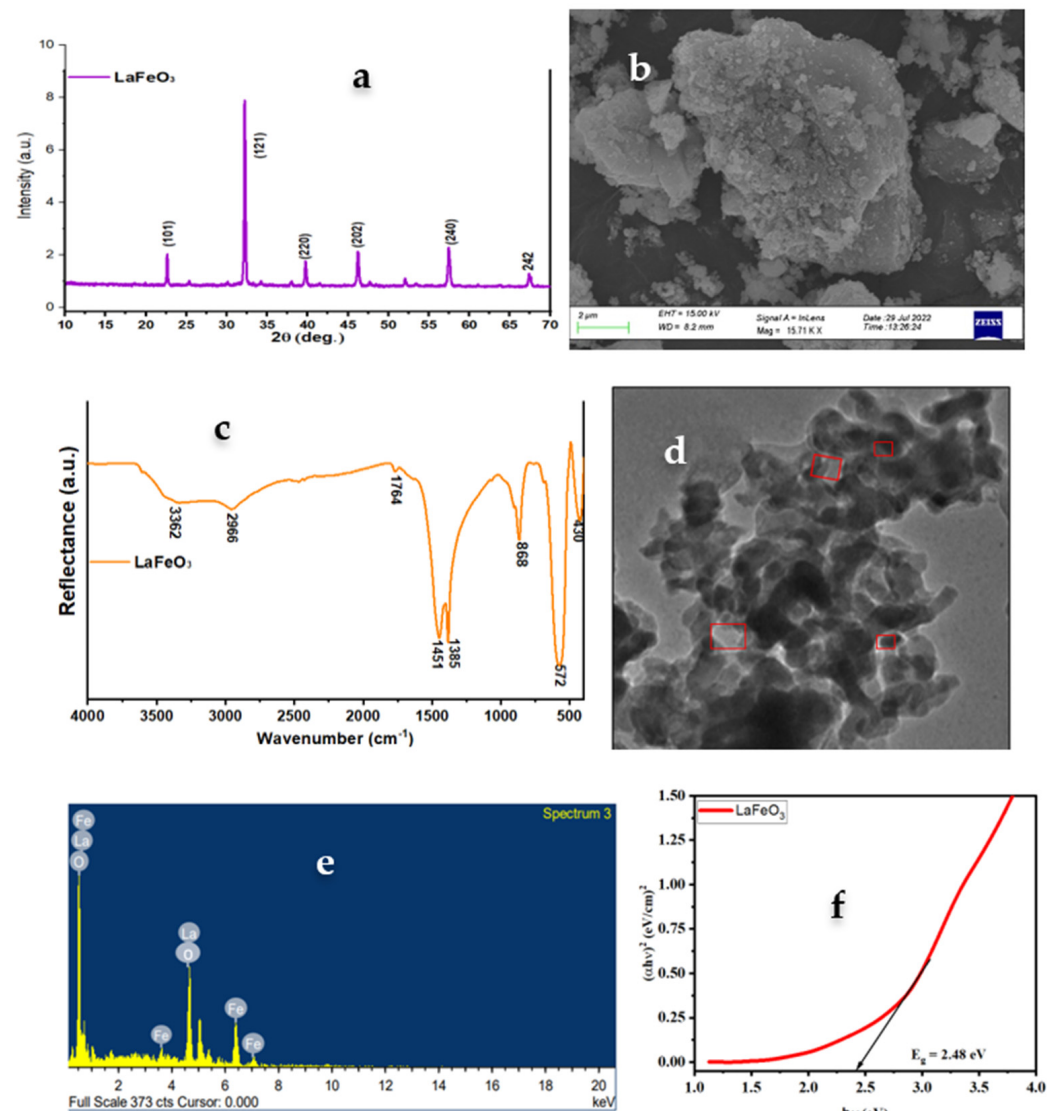


Figure 1. (a) XRD spectrum, (b) SEM image, (c) FTIR spectrum, (d) TEM image, (e) EDX, and (f) Tauc plot of the synthesized LaFeO_3 nanostructure.

3.2. Photocatalytic Activity of LaFeO_3 Nanostructures

The degradation percentage of MG was 82% in 80 min, as depicted in Figure 2a,b. Due to an increase in reactive site, charge transfer across the interfaces, and efficient absorption of visible light. Then, 30 mg catalyst was dispersed in 60 mL of MG (10 PPM) dye solution and maintained at constant stirring under sunlight. The 3 mL solution is removed at intervals of 5 min from the sample for the UV-Vis study. Equation (1) was used to calculate the percentage of malachite green absorbed on the catalyst surface [24,25].

$$\text{Percentage of degradation} = \frac{c_0 - c_t}{c_0} \times 100 \quad (1)$$

where c represents the initial time in absorption and c_t represents the absorption minutes.

The Photodegradation Mechanism of MG is depicted in Figure 3a. An upsurge in MG adsorption on the LaFeO_3 nanostructure surface might have reacted with reactive oxygen species (ROS) in the photocatalysis procedure. When LaFeO_3 was treated by visible light irradiated hole and electron pairs were created on the valence band (VB) and conduction band (CB) of the LaFeO_3 photocatalyst (Equation (2)). An electron on the conduction band generates superoxide (Equation (3)). Superoxide reacts with water and generates hydroxyl

radical (Equation (4)). In continuation, the hole can also react with the hydroxyl group from water generates $\bullet\text{OH}$ radicals (Equation (5)) [26,27]. The hydroxy radicals react with the dye and degrade the dye into CO_2 and H_2O as depicted in Figure 3b. The kinetics of photodegradation was 0.00356 min^{-1} .

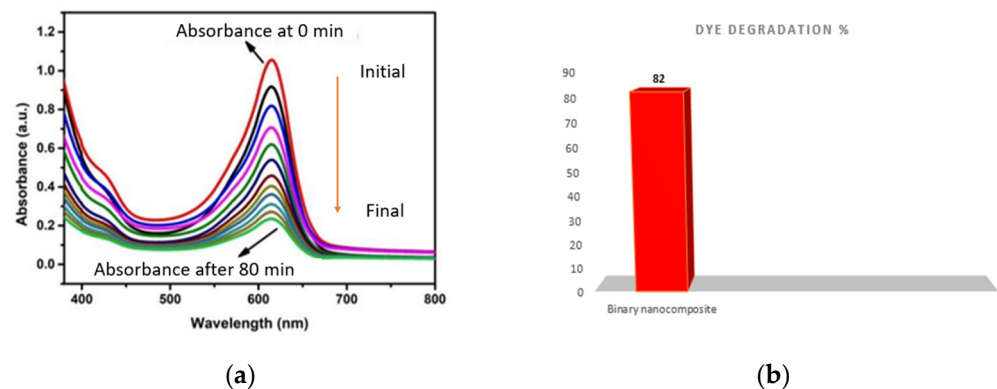
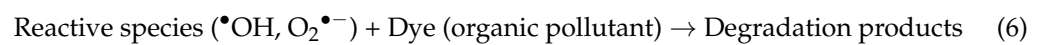
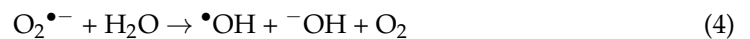
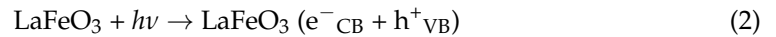


Figure 2. (a) Photodegradation of malachite green dye in aqueous solution under visible light for LaFeO_3 . (b) Bar graph representing dye degradation percentage. Different colours represent absorbance at different time period.

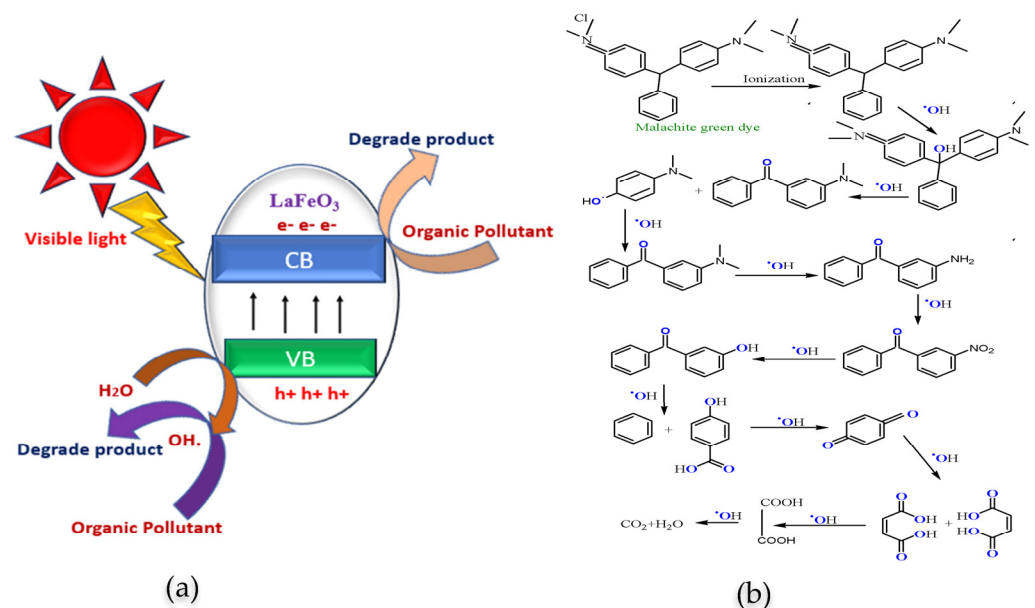


Figure 3. (a) Photocatalytic mechanism of synthesized nanocomposite. (b) Dye degradation steps involves reactive oxygen species.

The degradation percentage of MG is 82% due to an increase in reactive site, charge transfer across the interfaces, and efficient absorption of visible light [28].

4. Conclusions

Synthesis of LaFeO₃ nanostructure has been successfully performed by the Hydrothermal method. The LaFeO₃ nanostructure composite has high photocatalytic activity in the removal and degradation (82%) of the dye in 80 min, due to the large surface area, small band gap, and fast charge transference character. LaFeO₃ nanostructure, it could be utilized as a nano photocatalyst for wastewater remediation and can be further explored in heterojunction formation.

Author Contributions: Conceptualization, T.K. and S.B.; methodology, T.K., S.B. and A.S.G.; investigation and formal analysis, S.J.; writing, S.J. and T.K.; original draft preparation, S.J.; supervision, T.K. and S.B. All authors have read and agreed to the published version of the manuscript.

Funding: No external funding was availed for the study.

Institutional Review Board Statement: Not applicable.

Informed Consent Statement: Not applicable.

Data Availability Statement: The data associated with the study has been included in the paper.

Acknowledgments: The authors are thankful to A.R. Khan, Head, Department of Chemistry, Integral University, Lucknow and A. Mishra, Head, Department of Chemistry, University of Lucknow for the support. They are also thankful to the R&D cell of the University for providing the Manuscript Communication Number (IU/R&D/2022-MCN0001714). The authors also acknowledge the the USIF, Aligarh Muslim University, Aligarh for providing analytical and microscopic facilities.

Conflicts of Interest: The authors declare no conflict of interest.

References

1. Stoumpos, C.C.; Malliakas, C.D.; Peters, J.A.; Liu, Z.; Sebastian, M.; Im, J.; Chasapis, T.C.; Wibowo, A.C.; Chung, D.Y.; Freeman, A.J.; et al. Crystal Growth of the perovskite semiconductor CsPbBr₃: A material for high energy radiation detection. *Cryst. Growth Des.* **2013**, *13*, 2722–2727. [\[CrossRef\]](#)
2. Jabeen, S.; Ganie, A.S.; Hijazi, S.; Bala, S.; Bano, D.; Khan, T. Fabrication and studies of LaFe₂O₃/Sb₂O₃ heterojunction for enhanced degradation of Malachite green dye under visible light irradiation. *Inorg. Chem. Commun.* **2023**, *152*, 110729. [\[CrossRef\]](#)
3. Martynenko, I.V.; Litvin, A.P.; Purcell-Milton, F.; Baranov, A.V.; Fedorov, A.V.; Gun'ko, Y.K. Application of semiconductor quantum dots in bioimaging and biosensing. *J. Mater. Chem. B* **2017**, *5*, 6701–6727. [\[CrossRef\]](#) [\[PubMed\]](#)
4. Manser, J.S.; Christians, J.A.; Kamat, P.V. Intriguing optoelectronic properties of metal halide perovskites. *Chem. Rev.* **2016**, *116*, 12956–13008. [\[CrossRef\]](#)
5. Dursun, I.; Shen, C.; Parida, M.R.; Pan, J.; Sarmah, S.P.; Priante, D.; Alyami, N.; Liu, J.; Saidaminov, M.I.; Alias, M.S.; et al. Perovskite nanocrystals as a color converter for visible light communication. *ACS Photonics* **2016**, *3*, 1150–1156. [\[CrossRef\]](#)
6. Sercel, P.C.; Lyons, J.L.; Wickramaratne, D.; Vaxenburg, R.; Bernstein, N.; Efros, A.L. Exciton Fine Structure in Perovskite Nanocrystals. *Nano Lett.* **2019**, *19*, 4068–4077. [\[CrossRef\]](#) [\[PubMed\]](#)
7. Gong, S.; Xie, Z.; Li, W.; Wu, X.; Han, N.; Chen, Y. Highly active and humidity resistive perovskite LaFeO₃ based catalysts for efficient ozone decomposition. *Appl. Catal. B Environ.* **2019**, *241*, 578–587. [\[CrossRef\]](#)
8. Liu, A.; Bonato, L.G.; Sessa, F.; Almeida, D.B.; Isele, E.; Nagamine, G.; Zagonel, L.F.; Nogueira, A.F.; Padilha, L.A.; Cundiff, S.T. Effect of dimensionality on the optical absorption properties of CsPbI₃ perovskite nanocrystals. *J. Chem. Phys.* **2019**, *151*, 191103. [\[CrossRef\]](#)
9. Chen, D.; Wang, Q.; Shen, G.; Wang, R.; Shen, G. Ternary oxide nanostructured materials for supercapacitors: A review. *J. Mater. Chem. A Mater. Energy Sustain.* **2015**, *3*, 10158–10173. [\[CrossRef\]](#)
10. Rovisco, A.; Branquinho, R.; Martins, J.; Fortunato, E.; Martins, R.; Barquinha, P. Growth Mechanism of Seed-Layer Free ZnSnO₃ Nanowires: Effect of Physical Parameters. *Nanomaterials* **2019**, *9*, 1002. [\[CrossRef\]](#)
11. Peng, K.; Fu, L.; Yang, H.; Ouyang, J. Perovskite LaFeO₃/montmorillonite nanocomposites: Synthesis, interface characteristics and enhanced photocatalytic activity. *Sci. Rep.* **2016**, *6*, 19723. [\[CrossRef\]](#) [\[PubMed\]](#)
12. Shen, H.; Xue, T.; Wang, Y.; Cao, G.; Lu, Y.; Fang, G. Photocatalytic property of perovskite LaFeO₃ synthesized by sol-gel process and vacuum microwave calcination. *Mater. Res. Bull.* **2016**, *84*, 15–24. [\[CrossRef\]](#)
13. Jabeen, S.; Ahmad, N.; Bala, S.; Bano, D.; Khan, T. Nanotechnology in environmental sustainability and performance of nanomaterials in recalcitrant removal from contaminated Water: A review. *Int. J. Nano Dimens.* **2023**, *14*, 1–28.

14. Zhang, Q.; Huang, Y.; Peng, S.; Zhang, Y.; Shen, Z.; Cao, J.J.; Pui, D.Y. Perovskite LaFeO₃-SrTiO₃ composite for synergistically enhanced NO removal under visible light excitation. *Appl. Catal. B Environ.* **2017**, *204*, 346–357. [\[CrossRef\]](#)
15. Afifah, N.; Saleh, R. Enhancement of photocatalytic activities of perovskite LaFeO₃ composite by incorporating nanographene platelets. *IOP Conf. Ser. Mater. Sci. Eng.* **2017**, *188*, 012054. [\[CrossRef\]](#)
16. Gong, C.; Zhang, Z.; Lin, S.; Wu, Z.; Sun, L.; Ye, C.; Lin, C. Electrochemical synthesis of perovskite LaFeO₃ nanoparticle-modified TiO₂ nanotube arrays for enhanced visible-light photocatalytic activity. *New J. Chem.* **2019**, *43*, 16506–16514. [\[CrossRef\]](#)
17. Phuong, D.V. Photocatalytic Activity of Sr-doped LaCoO₃ Under UV Illumination. *Univ. Danang J. Sci. Technol.* **2015**, *6*, 42–45.
18. Khalil, K.M.; Mahmoud, A.H.; Khairy, M. Formation and textural characterization of size-controlled LaFeO₃ perovskite nanoparticles for efficient photocatalytic degradation of organic pollutants. *Adv. Powder Technol.* **2022**, *33*, 103429. [\[CrossRef\]](#)
19. Tuna, Ö.; Simsek, E.B. Anchoring LaFeO₃ perovskites on the polyester filters for flowthrough photocatalytic degradation of organic pollutants. *J. Photochem. Photobiol.* **2021**, *418*, 113405. [\[CrossRef\]](#)
20. Jayanthi, G.; Sumathi, S.; Kannan, K.; Andal, V.; Murugan, S. A Review on Synthesis, Properties, and Environmental Application of Fe-Based Perovskite. *Adv. Mater. Sci. Eng.* **2022**, *2022*, 6607683. [\[CrossRef\]](#)
21. Rezanezhad, A.; Rezaie, E.; Ghadimi, L.S.; Hajalilou, A.; Abouzari-Lotf, E.; Arsalani, N. Outstanding supercapacitor performance of Nd-Mn co-doped perovskite LaFeO₃@ nitrogen-doped graphene oxide nanocomposites. *Electrochim. Acta* **2020**, *335*, 135699. [\[CrossRef\]](#)
22. Vidyarajan, N.; Alexander, L.K. Strain induced optical properties of perovskite LaFeO₃. *Mater. Res. Express* **2018**, *6*, 015610. [\[CrossRef\]](#)
23. Thirumalairajan, S.; Girija, K.; Mastelaro, V.R.; Ponpandian, N. Investigation on magnetic and electric properties of morphologically different perovskite LaFeO₃ nanostructures. *J. Mater. Sci. Mater. Electron.* **2015**, *26*, 8652–8662. [\[CrossRef\]](#)
24. Abazari, R.; Sanati, S.; Saghatforoush, L.A. A unique and facile preparation of lanthanum ferrite nanoparticles in emulsion nanoreactors: Morphology, structure, and efficient photocatalysis. *Mater. Sci. Semicond. Process.* **2014**, *25*, 301–306. [\[CrossRef\]](#)
25. Yulizar, Y.; Apriandanu, D.O.B.; Ashna, R.I. La₂CuO₄-decorated ZnO nanoparticles with improved photocatalytic activity for malachite green degradation. *Chem. Phys. Lett.* **2020**, *755*, 137749. [\[CrossRef\]](#)
26. Collu, D.A.; Carucci, C.; Piludu, M.; Parsons, D.F.; Salis, A. Aurivillius oxides nanosheets-based photocatalysts for efficient oxidation of malachite green dye. *Int. J. Mol. Sci.* **2022**, *23*, 5422. [\[CrossRef\]](#) [\[PubMed\]](#)
27. Nakhoshtin Panahi, P.; Rasoulifard, M.H.; Babaei, S. Photocatalytic activity of cation (Mn) and anion (N) substitution in LaCoO₃ nanoperovskite under visible light. *Rare Metals* **2020**, *39*, 139–146. [\[CrossRef\]](#)
28. Deshmukh, V.V.; Ravikumar, C.R.; Kumar, M.A.; Ghotekar, S.; Kumar, A.N.; Jahagirdar, A.A.; Murthy, H.A. Structure, morphology and electrochemical properties of SrTiO₃ perovskite: Photocatalytic and supercapacitor applications. *Environ. Toxicol. Chem.* **2021**, *3*, 241–248. [\[CrossRef\]](#)

Disclaimer/Publisher's Note: The statements, opinions and data contained in all publications are solely those of the individual author(s) and contributor(s) and not of MDPI and/or the editor(s). MDPI and/or the editor(s) disclaim responsibility for any injury to people or property resulting from any ideas, methods, instructions or products referred to in the content.